Letter

Epidemic paradox induced by awareness driven network dynamics

Csegő Balázs Kolok [1,2] Gergely Ódor [3,2] Dániel Keliger [2,4] and Márton Karsai [3,2]
[1]Institute of Mathematics, Faculty of Science, ELTE Eötvös Loránd University, 1117 Budapest, Hungary
[2]National Laboratory of Health Security, HUN-REN Alfréd Rényi Institute of Mathematics, 1053 Budapest, Hungary
[3]Department of Network and Data Science, Central European University, 1010 Vienna, Austria
[4]Department of Stochastics, Institute of Mathematics, Budapest University of Technology and Economics, 1111 Budapest, Hungary

(Received 31 July 2024; accepted 5 February 2025; published 10 March 2025)

We study stationary epidemic processes in scale-free networks with local-awareness behavior adopted by only susceptible, only infected, or all nodes. We find that, while the epidemic size in the susceptible-aware and the all-aware models scales linearly with the network size, the scaling becomes sublinear in the infected-aware model. Hence, fewer aware nodes may reduce the epidemic size more effectively; a phenomenon reminiscent of Braess's paradox. We present numerical and theoretical analysis and highlight the role of influential nodes and their disassortativity to raise epidemic awareness.

DOI: 10.1103/PhysRevResearch.7.L012061

Epidemics drive substantial changes in human behavior, affecting our everyday lives, social interactions, and economic activities [1,2]. Most recently, amid the COVID-19 pandemic, people have heightened their protective measures [3,4], including mask wearing [5], increased hygiene practices [6], social distancing [7,8], and the avoidance of large gatherings [9,10]. These behavioral changes are intended to reduce disease transmission, which is often captured in behavior-disease—also called "awareness"—models [11–14].

In this Letter, we focus on a subtle, but powerful, form of awareness, called "local awareness" [15], which describes the behavioral changes adopted by individuals when they learn about an increase in the prevalence of the disease within their direct contacts, like among their family members or friends. In such situations, individuals may take preventive measures more seriously, causing a more substantial reduction in the disease transmission. Several models have been proposed to quantify the impact of local awareness in epidemic models [16–19], some of which were validated in real epidemic scenarios [20]. Our goal is to demonstrate how small changes in the awareness model—inspired by recent survey results—can cause substantial and even paradoxical changes in the resulting epidemic dynamics and outcome.

Our research design was inspired by the Hungarian MASZK COVID-19 questionnaire [21], where we asked respondents to rate their willingness to engage in local awareness, and their concern regarding their own health in case of an infection, on a scale of 1 to 5. Figure 1(a) shows that the respondents clustered into two distinct groups: those who rated both their health concerns and their awareness level high (5, 5), and those who rated their health concerns medium and their local awareness level high (3, 5). The former group contains predominantly middle-aged individuals, while the latter group contains predominantly older ones [Fig. 1(b)]. This observation is consistent with previous COVID-19 studies revealing different motivations to engage in protective behavior. In these survey experiments, younger people were found to be more concerned about infecting others while elder people tended to focus on protecting themselves [22,23]. It has also been shown that age is not the sole determining factor [24]; occupation and socioeconomic status may also influence motivations for protective behaviors.

To investigate the impact of motivational differences to engage in awareness behavior, we extend the susceptible-infected-susceptible (SIS) epidemic model with three distinct awareness models: (i) S-aware, where only the susceptible individuals are aware to protect their own health; (ii) I-aware, where only the infected individuals are aware to protect their peers; and (iii) SI-aware, where both susceptible and infected individuals engage in awareness behavior. While the effects of these awareness models have not been fully explored at the agent level, previous studies have shown that local awareness, in general, can raise the epidemic threshold [15,25–27], and I-awareness can reduce the epidemic size more effectively than S-awareness [11].

Going beyond these initial observations, our study aims to understand how awareness impacts the epidemic spreading dynamics in the three defined models. Our simulations reveal a counterintuitive result, showing that higher awareness levels can lead to larger epidemics, which is reminiscent of Braess's paradox [28]. The connection between epidemics and Braess's paradox has previously been made by Zhang *et al.* [29] in a game theoretic setting. In contrast, our result is an emergent network phenomenon, which we support by a theoretical analysis, a demonstration on real social networks, and an intuitive explanation of the metastable state of the SIS model in the three awareness scenarios.

Models and methods. Networks are defined by a set of nodes V and edges E, which represent connections between

Published by the American Physical Society under the terms of the Creative Commons Attribution 4.0 International license. Further distribution of this work must maintain attribution to the author(s) and the published article's title, journal citation, and DOI.

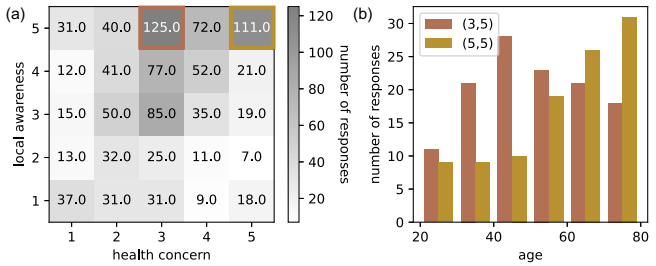


FIG. 1. (a) Two-dimensional histogram of local awareness and concerns of respondents about their own health in the case of an infection in the MASZK survey. The two most frequent answers are framed and written in white. (b) The age distribution of the two most frequent answers from panel (a). Among the most aware respondents, those who had medium health concerns (3) were middle-aged (red) and those who had the highest health concerns (5) were older (yellow).

the nodes. We focus on random networks with a power-law degree distribution generated by the Chung-Lu model [30,31], a generalization of the Erdős-Rényi model. In a network of size n, we add an edge between nodes i and j with the probability $w_{ij} := \kappa \frac{d_i d_j}{D}$, where $D = \sum_i d_i$ is a normalization term, $\kappa > 0$ is a density parameter, and d_i is a power-law sequence with the exponent γ [31]. Note that vertex i has the expected degree κd_i and that the second moment of the degree sequence is infinite for $\gamma \in (2, 3)$ and finite if $\gamma > 3$.

An SIS process assumes each network node to be either susceptible or infected. We initialize all nodes to be susceptible, except a small, randomly selected set of infected seed nodes. Thereafter, in each step, an infected node infects its susceptible neighbors with the probability β_0, while recovering with the probability μ. Eventually, the SIS process is known to reach a metastable state, where the number of infected individuals does not change beyond statistical fluctuations. We denote this metastable epidemic size by I_∞.

To introduce local awareness to the SIS model, we use an exponentially decaying awareness function inspired by the models of Refs. [15,32]. If an infected node u and a susceptible node v are connected by an edge, u infects v with the probability

$$\beta(u, v, t) = \beta_0 a(v, t)^{\alpha_S} a(u, t)^{\alpha_I}, \tag{1}$$

where $a(v, t) = e^{-N_I(v,t)}$ is the awareness function of an aware node v [function $a(u, t)$ has the same form], $N_I(v, t)$ denotes the number of infected neighbors of node v at time t, and the constants α_S and α_I determine the nature of the local-awareness model in the population. We discuss why the awareness function depends on the number and not the proportion of the infected neighbors in Sec. 1 of the Supplemental Material [33]. We distinguish three notable prevalence-based local-awareness models:

(i) S-aware (M_S), where $\alpha_S = 1$ and $\alpha_I = 0$ (only susceptible nodes are aware),

(ii) I-aware (M_I), where $\alpha_S = 0$ and $\alpha_I = 1$ (only infected nodes are aware),

(iii) SI-aware (M_{SI}), where $\alpha_S = \alpha_I = 1$ (infected nodes in the neighborhoods of both susceptible and infected nodes are aware).

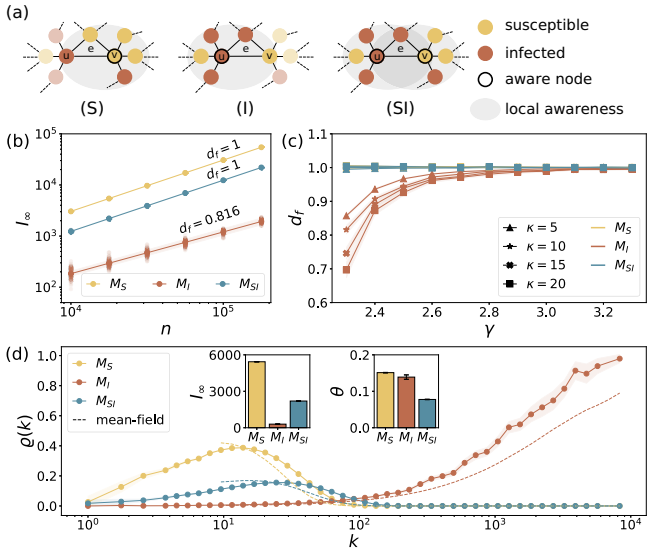


FIG. 2. (a) Illustration of the set of nodes (in shaded areas) counted in the exponents of the awareness functions in the (S) S-aware M_S, (I) I-aware M_I, and (SI) SI-aware M_{SI} models. (b) The fractal dimension d_f measured as the slope of the metastable epidemic size I_∞ as a function of the network size n in Chung-Lu networks with $\gamma = 2.3$ and $\kappa = 10$. (c) For the degree exponent $\gamma < 3$, the fractal dimension of the M_I model is smaller than 1, whereas the fractal dimensions of the M_S and M_{SI} models remain 1. Paradoxically, the infection becomes smaller in the M_I model despite that more nodes are aware in the M_{SI} model. (d) The density of infection in the metastable state $\varrho(k)$ as a function of the node degree k in both simulations (solid lines) and mean-field numerical approximations (dashed lines). Infection is concentrated on low-degree nodes in the M_S and M_{SI} models, while for the M_I model, the high-degree nodes dominate the infection. The inset on the left verifies that the metastable epidemic size is the lowest for the M_I model. The inset on the right shows no paradox in the perceived infection density θ, defined as the probability that a randomly chosen edge has an infected node on its end.

Figure 2(a) illustrates how the infected neighbors $N_I(u, t)$ and $N_I(v, t)$ are counted in the exponent of the infection probabilities of the three awareness models.

Results. Since more nodes are aware in the M_{SI} model compared to the M_S and M_I models, one would expect that the M_{SI} model would consistently lead to the lowest number of infected nodes. Interestingly, we find that this is not always the case.

To assess differences between the three models in a robust way, we measure the asymptotic growth of the metastable epidemic size I_∞ as a function of the network size n. More precisely, we assume the polynomial relation $I_\infty \sim n^{d_f}$, and we are interested in the exponent d_f, also called the fractal dimension of the metastable state. Numerically, d_f can be estimated by the slope of I_∞ as a function of n on a log-log plot [see Fig. 2(b)].

In supercritical SIS models without awareness, the metastable infection size I_∞ is known to be linear in the network size [34], which means that the fractal dimension attains its maximum value ($d_f = 1$). Figure 2(c) shows that the same is true for the M_S and M_{SI} models, across all values

of γ, suggesting that these awareness mechanisms are unable to asymptotically reduce the epidemic size. However, surprisingly, Fig. 2(c) also shows that the M_{I} model has a fractal dimension strictly less than 1, implying sublinear growth, for networks with $\gamma < 3$. In this context, sublinearity means that, for large enough networks, the density of infectious individuals in the stationary state can be lower than any fixed number, in particular, lower than the stationary infection densities in the M_{S} and M_{SI} models. This is a highly counterintuitive result: even though less nodes are aware in the M_{I} model, the epidemic becomes smaller compared to the M_{SI} model, when all nodes reduce contacts [Fig. 2(d), left inset]. Additionally, as the network density κ increases, the fractal dimension further decreases in the M_{I} model, strengthening the paradoxical phenomenon.

Figure 2(d) shows that the three awareness models lead to markedly different degree profiles among the infected nodes, hinting at an intuitive explanation of the paradox. In the M_{S} and M_{SI} models, the infection density is highest among low-degree nodes (degrees between 10 and 50), and since they constitute the overwhelming majority of the network, the epidemic size is also high. In contrast, in the M_{I} model, the infection is concentrated on the high-degree nodes (degrees larger than 1000), and low-degree nodes remain sparsely infected, making the infection size significantly smaller. In other words, even though the M_{SI} model has the highest potential to reduce the epidemic size, due to the way the epidemic is distributed in the metastable state, awareness has a bigger impact in the M_{I} model.

We observe no paradoxical behavior if we evaluate the infection density "perceived" by the nodes, defined as the fraction of infected neighbors θ of a randomly chosen individual. Indeed, the second inset of Fig. 2(d) shows that θ is smallest for the M_{SI} model. This observation suggests that in the M_{I} model, a few infected high-degree nodes increase the perceived epidemic density in their large neighborhoods, serving as "warning examples" and protecting the rest of the population from the disease. However, if these nodes are more interested in protecting themselves, as in the case of the M_{SI} and M_{S} models, then high-degree nodes do not become infected and, therefore, do not alert their neighbors; instead they are essentially removed from the network. Although the removal of high-degree nodes does slow down the epidemic propagation compared to a null model without awareness, the network between the low-degree nodes remains intact, and a constant fraction of nodes become infected in the stationary state. Eventually, the perceived epidemic density becomes comparable in all three behavior-epidemic models, however, this means a significantly higher number of infected low-degree nodes in the M_{SI} and M_{S} models, compared to the few infected hubs in the M_{I} model.

We also observe no paradoxical behavior in the first few time-steps of the three awareness models, initialized from the same seed nodes. Instead, high-degree nodes become infected first in all three models [Supplemental Material [33], Sec. 6], and the epidemic grows slowest in the M_{SI} model [Supplemental Material [33], Fig. A.1(a)], as expected from the increased awareness level. However, these local dynamics quickly become dominated by the global metastable state, where an increased capacity (higher awareness potential in the M_{SI} model) causes a worse overall performance (compared to the M_{I} model), similarly to Braess's paradox [28] in traffic flows.

Theoretical results. The observed awareness paradox and its intuitive explanation can be formalized and proved mathematically, confirming that it is a fundamental phenomenon in behavior-disease models. In this Letter, we focus on presenting the main results and insights, and for further details we refer the reader to the Supplemental Material [33], Secs. 3–5.

We obtain theoretical results by making two kinds of approximations on the underlying network and the stochastic process. First, we assume the network is annealed [35], namely, the adjacency matrix is replaced by the connection probabilities w_{ij}, modifying the awareness function a to

$$\hat{a}(i,t) := \exp\left(-\sum_j w_{ij}\hat{u}_j(t)\right), \tag{2}$$

where $\hat{u}_j(t)$ is the indicator of the vertex j being infected at time t. Analogously to Eq. (1), a susceptible vertex i gets infected at rate $\beta_0\hat{\phi}_i(t)$ in the annealed model, with

$$\hat{\phi}_i(t) = \hat{a}(i,t)^{\alpha_S}\sum_j w_{ij}\hat{a}(j,t)^{\alpha_I}\hat{u}_j(t). \tag{3}$$

Second, we apply the N-intertwined mean-field approximation [36] and assume that the states of the vertices are independent. The resulting closed system of ordinary differential equations (ODEs) can be expressed as

$$\frac{\mathrm{d}}{\mathrm{d}t}u_i(t) = -\mu u_i(t) + \beta_0\phi_i(t)[1-u_i(t)], \tag{4}$$

where the symbols without the hat symbol represent the mean-field approximation of the expectation of the quantities with the hat symbol. More explicitly, $u_i(t)$ approximates $\mathbb{E}[\hat{u}_i(t)]$, and $\phi_i(t)$ is analogous to $\hat{\phi}_i(t)$, with $\hat{u}_i(t)$ replaced by $u_i(t)$ in Eqs. (2) and (3).

After solving Eq. (4) (see derivation details at the end of this Letter, in the Appendixes), and setting the degree exponent $\gamma \in (2,3)$ and the density parameter $\kappa = n^{\delta}$ for some $0 \leqslant \delta \leqslant 1$, we arrive at our main theoretical result:

$$\begin{aligned} d_f^{\mathrm{SI}} &= 1-\delta, \\ d_f^{\mathrm{I}} &= 1-\frac{1}{\gamma-2}\delta. \end{aligned} \tag{5}$$

Indeed, Eq. (5) shows that the fractal dimension of the epidemic is strictly smaller in the M_{I} model compared to the M_{SI} model for heterogeneous [$\gamma \in (2,3)$] and dense ($\delta > 0$) degree distributions, proving the paradox.

Figure 3 confirms the agreement between the stochastic simulations, the numerical approximation, and Eq. (5). These quantitative results reinforce our previous observation, that the paradox appears in its strongest form in dense and degree heterogeneous networks. For further illustration, in Sec. 2 of the Supplemental Material [33], we show via simulations and theoretic analysis that the paradox is present in extremely heterogeneous starlike networks too.

Results on real networks. After demonstrating and understanding our counterintuitive result on synthetic Chung-Lu networks, we shift our focus towards real networks. We

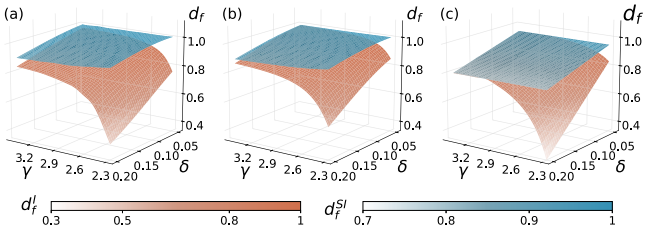


FIG. 3. The fractal dimension d_f of the infection size as a function of the degree distribution exponent γ and the average degree exponent δ in the I-aware and the SI-aware models is in agreement in (a) stochastic simulations, (b) mean-field numerical results, and (c) analytical results [Eq. (5)]. For $\gamma \in (2, 3)$, the fractal dimension in the I-aware model is strictly smaller than that in the SI-aware model in all three approaches.

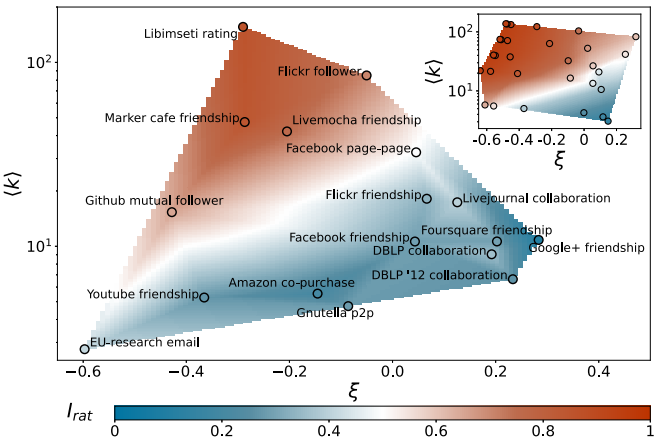


FIG. 4. The separation between paradox-exhibiting (red) and non-exhibiting (blue) real networks. The main plot shows I_{rat}, defined in Eq. (6), as a function of the average degree $\langle k \rangle$ and the degree assortativity ξ. We compute ξ by fitting the exponent of $k_{\text{nn}}(k) = ck^{\xi}$, where $k_{\text{nn}}(k)$ is the average neighbor degree of nodes with degree k [37]. If $\xi > 0$, the network is assortative; otherwise, it is disassortative. The continuous surface is fitted on the data points via linear interpolation. The upper inset shows a similar behavior on synthetically generated Chung-Lu networks with tunable assortativiy (see Sec. 8 in the Supplemental Material [33]).

gathered 17 real social and computer networks from publicly available datasets (see Supplemental Material [33], Table A.1). Stochastic simulations revealed that among these 17 networks, 5 exhibit the paradox (flickr follower, libmseti rating, livemocha friendship, marker cafe friendship, and github mutual follower). Based on our results in synthetic networks, we expect that the two main network characteristics that distinguish these 5 networks from the other 12 are average degree and degree heterogeneity. Indeed, when we plot the ratio of the infection size in the two models,

$$I_{\text{rat}} = \frac{I_{\text{SI}}}{I_{\text{I}} + I_{\text{SI}}}, \tag{6}$$

as a function of the average degree and the standard deviation of the degree distribution, there is a clear separation between the 5 paradox-exhibiting and the 12 non-exhibiting networks (see Supplemental Material [33], Fig. A.4). However, if we employ a degree-preserving random shuffling of the edges, the paradox appears in 5 additional networks [see Supplemental Material [33], Fig. A.4(b)], suggesting that network characteristics beyond the degree distribution play a role in the appearance of the paradox.

According to our previous results, the key mechanism responsible for the paradox is the infected hubs inducing awareness in low-degree nodes. However, many real networks are assortative, which means that low-degree nodes are less likely to connect to hubs, weakening the paradox. Indeed, plotting the ratio I_{rat} in Fig. 4 as a function of the average degree $\langle k \rangle$ and the assortativity parameter ξ (defined in the figure legend), we see a clear separation for both real (main) and synthetic networks (upper inset). This result suggests that disassortativty is a key network characteristic that contributes to the paradox arising, although dense enough assortative networks still exhibit the phenomenon (Fig. 4, upper inset).

Finding all network characteristics that may contribute to the paradox is outside the scope of this Letter. However, both the mathematical proof and the data analysis suggest that network density, disassortativity, and degree heterogeneity are the three most important properties, while other characteristics (e.g., clustering coefficient) play a smaller role (see Supplemental Material [33], Table A.2).

Conclusion. In this Letter, we demonstrated a highly counterintuitive result about the interplay of disease propagation and awareness behavior; *fewer* potentially aware nodes may be *more* effective in containing an epidemic, due to a *sublinear* population size dependency of stationary epidemic size, in case only infected nodes are aware. This is a more effective strategy than *any* other preventive measure, which permits a linear epidemic size (e.g., other types of local awareness, global awareness, government regulations, etc.). The observed paradox reinforces that awareness behavior has the greatest societal benefit when focused on protecting others, as shown for the epidemic threshold earlier [11]. However, instead of thresholds, by focusing on the metastable epidemic size, we provide a very different explanation in nature. We reveal that the paradox is induced by the interaction between human behavior and the disease distribution within the population, calling for epidemic behavioral surveillance efforts during pandemics beyond reporting the effective reproductive number or sheer case numbers.

Although our observations are motivated by surveys, and demonstrated by simulations and mathematical analysis, they have limitations. The implemented awareness models are only a crude approximation of reality. They assume that all individuals employ the same awareness function, while awareness may depend on individual features [38]. A more detailed exploration of the interactions between human behavior and epidemics could be the target of future works. Nevertheless, the fact that the epidemic size is *asymptotically* smaller in the I-aware model compared to the S and SI-aware models, with various real networks exhibiting similar behavior, suggests that the paradox is robust against our modeling choices.

Further, the degree distribution of real contact networks is often more uniform than the assumed power-law scaling. Moreover, the information about the disease may not be transmitted on the same contact network where the disease spreads.

Nevertheless, we believe the paradox will persist in multiplex networks with a more homogeneous contact layer and a scale-free information layer [39–41], a topic which remains for future research.

Perhaps our most important message is the delicate role of influential nodes on the long-term dynamics of an epidemic. Asymmetries in the local update rule and the presence of hubs have already been shown to produce surprising results in the case of the voter model [42]. In epidemic models, Zhang *et al.* [32] reported that influential nodes can act as a "double-edged sword" by either speeding up or slowing down the disease propagation depending on whether they transmit the disease or the information about the disease at a faster rate. We complement these findings by understanding how different motivations to engage in awareness behavior change the role of influential nodes. We show that, if hub nodes are primarily interested in protecting others, they are able to increase the perceived infection density in the population, leading to an awareness response that controls the epidemic more effectively than in scenarios where hubs are primarily motivated by self-protective behaviors. We believe that, besides a deeper mathematical understanding of the phenomenon, this finding will inspire future modeling, and it will guide information campaigns in epidemic prevention and crisis management.

Acknowledgments. We acknowledge Z. Király, B. Ráth, M. Abért, and L. Lovász for their scientific contributions and thank J. Koltai and G. Röst for their contribution to the MASZK data collection. C.B.K. and M.K. were supported by the National Laboratory for Health Security (Grant No. RRF-2.3.1-21-2022-00006); G.Ó. was supported by the Swiss National Science Foundation (Grant No. P500PT-211129); and M.K. was supported by the CHIST-ERA project (SAI: FWF I 5205-N), the SoBigData++ H2020-871042, and the SoBigData-PPP HORIZON-INFRA-2021-DEV-02 program (Grant No. 101079043).

Appendix. In this section, we provide additional insights for specialists on our theoretical results.

For sequences a_n and b_n, we use the notation $a_n \sim b_n$ to denote $a_n/b_n = 1 + o(1)$ and the notation $a_n \asymp b_n$ to denote $a_n = \Theta(b_n)$, (big Θ is the notation of asymptotical behavior and should not be confused with small θ, our notation for the perceived infection density). Whenever we take limits, we first let $n \to \infty$ and then let $\kappa \to \infty$. Since the paradox only involves the M_{SI} and M_{I} models, we assume $\alpha_I > 0$ in the analytic derivations.

We are interested in finding the nonzero steady state of Eq. (4), which we prove is unique in Lemma A.1. in the Supplemental Material [33] and we denote by u_i. Interestingly, to solve this system of ODEs, we first have to understand the infection density perceived by the nodes or, in other words, the probability of a randomly selected stub being infected in the mean-field model, defined by

$$\theta = \frac{1}{D}\sum_i d_i u_i.$$

Solving the system of mean-field equations (detailed derivation in Lemmas A.3 and A.4 and Remark A.1 in the Supplemental Material [33]), the asymptotic behavior of θ can be expressed as

$$\theta \sim \frac{1}{\alpha_S + \alpha_I}\frac{\log\kappa}{\kappa}. \tag{A1}$$

This result agrees with the second inset of Fig. 2(d) and with the intuition that a higher $\alpha_S + \alpha_I$ should result in a lower infection density at least in the "perceived" sense. Next, we show that, while the perceived infection density is a good proxy for the epidemic size in certain cases, the epidemic size can be significantly lower in others, inducing the paradox.

When mainly low-degree vertices are infected, the normalized epidemic size I_∞/D and the perceived epidemic density θ are comparable. In fact, θ upper bounds I_∞/D as

$$\theta = \frac{1}{D}\sum_i d_i u_i \geqslant \frac{1}{D}\sum_i u_i = \frac{1}{D} I_\infty. \tag{A2}$$

In Eq. (A2), equality holds if and only if $u_i = 0$ for all i larger than 1, i.e., if only the lowest-degree nodes are infected. As we saw in Fig. 2(d), this is approximately true in the M_{SI} model, suggesting that for this awareness model, inequality Eq. (A2) is asymptotically sharp. We formalize this intuition (see details in Lemma A.10 in the Supplemental Material [33]) mathematically as

$$I_\infty^{\mathrm{SI}} \sim D\theta_{\mathrm{SI}} \asymp n\theta_{\mathrm{SI}}. \tag{A3}$$

In contrast, in the M_{I} model, the infection probabilities u_i increase for larger degrees, potentially making the inequality Eq. (A2) loose, and therefore I_∞^{I} is asymptotically smaller than I_∞^{SI}. Indeed, we show that the tightness of inequality Eq. (A2) undergoes a phase transition in the degree exponent, and the critical threshold is at $\gamma = 3$, where the second moment of the degree distribution becomes infinite. More precisely (derivation in Remark A.2 of the Supplemental Material [33]), we can write the asymptotic behavior of the number of infected individuals in the M_{I} model as

$$I_\infty^{\mathrm{I}} \asymp \begin{cases} n\theta_{\mathrm{I}} & \text{if } 3 < \gamma, \\ n\theta_{\mathrm{I}}^{\frac{1}{\gamma-2}} & \text{if } 2 < \gamma < 3. \end{cases} \tag{A4}$$

Since $\theta_{\mathrm{I}} \asymp \theta_{\mathrm{SI}} \to 0$ as $\kappa \to \infty$, I_∞^{I} is indeed asymptotically smaller than I_∞^{SI} in the range $\gamma \in (2, 3)$; in particular, for large enough networks, we have $I_\infty^{\mathrm{I}} < I_\infty^{\mathrm{SI}}$, proving the paradoxical result.

Moreover, we are able to quantify the fractal dimension in the M_{I} and M_{SI} models as a function of the degree exponent and the average degree. Setting $\gamma \in (2, 3)$ and $\kappa = n^\delta$ for some $0 \leqslant \delta \leqslant 1$, and combining Eqs. (A1), (A3), and (A4), we arrive at our main theoretical result expressing the fractal dimensions in Eq. (5).

[1] V. L. Champion and C. S. Skinner, The health belief model, in *Health Behavior and Health Education: Theory, Research, and Practice*, 4th ed., edited by K. Glanz, B. K. Rimer, and K. Viswanath (Jossey-Bass, San Francisco, 2008), pp. 45–66.

[2] C. Abraham and P. Sheeran, The health belief model, in *Predicting Health Behaviour: Research and Practice with Social Cognition Models*, 2nd ed., edited by M. Conner and P. Norman (Open University, Buckingham, England, 2005), p. 30.

[3] R. Jose, M. Narendran, A. Bindu, N. Beevi, M. L, and P. Benny, Public perception and preparedness for the pandemic COVID 19: A health belief model approach, Clin. Epidemiol. Global Health **9**, 41 (2021).

[4] P. Borkowski, M. Jażdżewska-Gutta, and A. Szmelter-Jarosz, Lockdowned: Everyday mobility changes in response to COVID-19, J. Transp. Geogr. **90**, 102906 (2021).

[5] M. H. Haischer, R. Beilfuss, M. R. Hart, L. Opielinski, D. Wrucke, G. Zirgaitis, T. D. Uhrich, and S. K. Hunter, Who is wearing a mask? Gender-, age-, and location-related differences during the COVID-19 pandemic, PLoS ONE **15**, e0240785 (2020).

[6] J. Gibson Miller, T. K. Hartman, L. Levita, A. P. Martinez, L. Mason, O. McBride, R. McKay, J. Murphy, M. Shevlin, T. V. Stocks *et al.*, Capability, opportunity, and motivation to enact hygienic practices in the early stages of the COVID-19 outbreak in the United Kingdom, Br. J. Health Psychol. **25**, 856 (2020).

[7] S. Gupta, K. I. Simon, and C. Wing, Mandated and Voluntary Social Distancing During The COVID-19 Epidemic: A Review, Working Paper 28139, National Bureau of Economic Research, 2020.

[8] M. Andersen, Early evidence on social distancing in response to COVID-19 in the United States (April 5, 2020). Available at SSRN https://ssrn.com/abstract=3569368 or http://dx.doi.org/10.2139/ssrn.3569368.

[9] S. H. Ebrahim and Z. A. Memish, COVID-19—the role of mass gatherings, Travel Med. Infect. Dis. **34**, 101617 (2020).

[10] G. St-Onge, V. Thibeault, A. Allard, L. J. Dubé, and L. Hébert-Dufresne, Social confinement and mesoscopic localization of epidemics on networks, Phys. Rev. Lett. **126**, 098301 (2021).

[11] S. Funk, M. Salathé, and V. A. Jansen, Modelling the influence of human behaviour on the spread of infectious diseases: a review, J. R. Soc. Interface **7**, 1247 (2010).

[12] Z. Wang, M. A. Andrews, Z.-X. Wu, L. Wang, and C. T. Bauch, Coupled disease–behavior dynamics on complex networks: A review, Phys. Life Rev. **15**, 1 (2015).

[13] F. Verelst, L. Willem, and P. Beutels, Behavioural change models for infectious disease transmission: A systematic review (2010–2015), J. R. Soc. Interface **13**, 20160820 (2016).

[14] A. Teslya, T. M. Pham, N. G. Godijk, M. E. Kretzschmar, M. C. Bootsma, and G. Rozhnova, Impact of self-imposed prevention measures and short-term government-imposed social distancing on mitigating and delaying a COVID-19 epidemic: A modelling study, PLoS Med. **17**, e1003166 (2020).

[15] Q. Wu, X. Fu, M. Small, and X.-J. Xu, The impact of awareness on epidemic spreading in networks, Chaos **22**, 013101 (2012).

[16] T. Gross, C. J. D. D'Lima, and B. Blasius, Epidemic dynamics on an adaptive network, Phys. Rev. Lett. **96**, 208701 (2006).

[17] S. Funk, E. Gilad, C. Watkins, and V. A. Jansen, The spread of awareness and its impact on epidemic outbreaks, Proc. Natl. Acad. Sci. USA **106**, 6872 (2009).

[18] I. Z. Kiss, J. Cassell, M. Recker, and P. L. Simon, The impact of information transmission on epidemic outbreaks, Math. Biosci. **225**, 1 (2010).

[19] N. Perra, D. Balcan, B. Gonçalves, and A. Vespignani, Towards a characterization of behavior-disease models, PloS ONE **6**, e23084 (2011).

[20] G. Ódor and M. Karsai, Epidemic-induced local awareness behavior inferred from surveys and genetic sequence data, arXiv:2406.09983.

[21] M. Karsai, J. Koltai, O. Vasarhelyi, and G. Röst, Hungary in mask/maszk in Hungary, Corvinus J. Sociol. Soc. Policy **11**, 139 (2020).

[22] A. Shiina, T. Niitsu, O. Kobori, K. Idemoto, T. Hashimoto, T. Sasaki, Y. Igarashi, E. Shimizu, M. Nakazato, K. Hashimoto *et al.*, Relationship between perception and anxiety about COVID-19 infection and risk behaviors for spreading infection: A national survey in Japan, Brain, Behav., Immun.–Health **6**, 100101 (2020).

[23] A. Germani, L. Buratta, E. Delvecchio, and C. Mazzeschi, Emerging adults and COVID-19: The role of individualism-collectivism on perceived risks and psychological maladjustment, Int. J. Environ. Res. Public Health **17**, 3497 (2020).

[24] S. Pappa, N. Athanasiou, N. Sakkas, S. Patrinos, E. Sakka, Z. Barmparessou, S. Tsikrika, A. Adraktas, A. Pataka, I. Migdalis *et al.*, From recession to depression? Prevalence and correlates of depression, anxiety, traumatic stress and burnout in healthcare workers during the COVID-19 pandemic in Greece: A multi-center, cross-sectional study, Int. J. Environ. Res. Public Health **18**, 2390 (2021).

[25] F. D. Sahneh, F. N. Chowdhury, and C. M. Scoglio, On the existence of a threshold for preventive behavioral responses to suppress epidemic spreading, Sci. Rep. **2**, 632 (2012).

[26] C. Liu, J.-R. Xie, H.-S. Chen, H.-F. Zhang, and M. Tang, Interplay between the local information based behavioral responses and the epidemic spreading in complex networks, Chaos **25**, 103111 (2015).

[27] A. Moinet, R. Pastor-Satorras, and A. Barrat, Effect of risk perception on epidemic spreading in temporal networks, Phys. Rev. E **97**, 012313 (2018).

[28] D. Braess, Über ein paradoxon aus der verkehrsplanung, Unternehmensforschung **12**, 258 (1968).

[29] H.-F. Zhang, Z. Yang, Z.-X. Wu, B.-H. Wang, and T. Zhou, Braess's paradox in epidemic game: Better condition results in less payoff, Sci. Rep. **3**, 3292 (2013).

[30] F. C. William Aiello and L. Lu, A random graph model for power law graphs, Exp. Math. **10**, 53 (2001).

[31] D. Fasino, A. Tonetto, and F. Tudisco, Generating large scale-free networks with the Chung–Lu random graph model, Networks **78**, 174 (2021).

[32] H.-F. Zhang, J.-R. Xie, M. Tang, and Y.-C. Lai, Suppression of epidemic spreading in complex networks by local information based behavioral responses, Chaos **24**, 043106 (2014).

[33] See Supplemental Material at http://link.aps.org/supplemental/10.1103/PhysRevResearch.7.L012061 for the simulation details and the step-by-step proof of the theoretical results.

[34] M. Newman, *Networks* (Oxford University, Oxford, 2018).

[35] S. C. Ferreira, R. S. Ferreira, and R. Pastor-Satorras, Quasistationary analysis of the contact process on annealed scale-free networks, Phys. Rev. E **83**, 066113 (2011).

[36] P. Mieghem, The N-intertwined SIS epidemic network model, Computing **93**, 147 (2011).

[37] R. Pastor-Satorras, A. Vázquez, and A. Vespignani, Dynamical and correlation properties of the internet, Phys. Rev. Lett. **87**, 258701 (2001).

[38] H. Xu, Y. Zhao, and D. Han, The impact of the global and local awareness diffusion on epidemic transmission considering the heterogeneity of individual influences, Nonlinear Dyn. **110**, 901 (2022).

[39] C. Granell, S. Gómez, and A. Arenas, Dynamical interplay between awareness and epidemic spreading in multiplex networks, Phys. Rev. Lett. **111**, 128701 (2013).

[40] E. Massaro and F. Bagnoli, Epidemic spreading and risk perception in multiplex networks: A self-organized percolation method, Phys. Rev. E **90**, 052817 (2014).

[41] J.-Q. Kan and H.-F. Zhang, Effects of awareness diffusion and self-initiated awareness behavior on epidemic spreading—An approach based on multiplex networks, Commun. Nonlinear Sci. Numer. Simul. **44**, 193 (2017).

[42] C. Castellano, Effect of network topology on the ordering dynamics of voter models, AIP Conf. Proc. **779**, 114 (2005).